

Treatment with Outgrowth Endothelial Cells Protects Cerebral Barrier against Ischaemic Injury

Rais Reskiawan A. Kadir, Mansour Alwjwaj,* Ulvi Bayraktutan**

**Academic Unit of Mental Health and Clinical Neuroscience, School of Medicine, The University of Nottingham*

Address for correspondence:

Associate Professor Ulvi Bayraktutan

Academic Unit of Mental Health and Clinical Neuroscience,

Clinical Sciences Building,

School of Medicine,

The University of Nottingham,

Hucknall Road,

Nottingham NG5 1PB,

United Kingdom.

Tel: +44-(115) 8231764

Fax: +44-(115) 8231767

E-mail: ulvi.bayraktutan@nottingham.ac.uk

Abstract

Background and aims: We have previously reported that outgrowth endothelial cells (OECs) restore cerebral endothelial cell integrity through effective homing to the injury site. This study further investigates whether treatment with OECs can restore blood-brain barrier (BBB) function in both *in vitro* and *in vivo* settings of ischaemia-reperfusion injury.

Methods: An *in vitro* model of human BBB was established by co-culture of astrocytes, pericytes, and human brain microvascular endothelial cells (HBMECs) before exposure to oxygen-glucose deprivation alone, or followed by reperfusion (OGD±R) in the absence or presence of exogenous OECs. Using a rodent model of middle cerebral artery occlusion (MCAO), we further assessed the therapeutic potential of OECs *in vivo*.

Results: Owing to their prominent anti-oxidant, proliferative, and migratory properties, alongside their inherent capacity to incorporate into brain vasculature, treatments with OECs attenuated the extent of OGD±R injury on BBB integrity and function, as ascertained by increases in transendothelial electrical resistance and decreases in paracellular flux across the barrier. Similarly, intravenous delivery of OECs also led to better barrier protection in MCAO rats as evidenced by significant decreases in ipsilateral brain oedema volumes on day 3 after treatment. Mechanistic studies subsequently showed that treatment with OECs substantially reduced oxidative stress and apoptosis in HBMECs subjected to ischaemic damages.

Conclusion: This experimental study has shown that OEC-based cell therapy restores BBB integrity in an effective manner by integrating into resident cerebral microvascular network, suppressing oxidative stress and cellular apoptosis.

Keywords: Endothelial progenitor cells, blood-brain barrier, stem cells, cell therapy, stroke, brain oedema

Introduction

Stroke is the third-leading cause of death and disability worldwide [1,2]. Despite being the main cause of human cerebral damage, thrombolysis with recombinant tissue plasminogen activator (rtPA) remains the only approved pharmacotherapy for ischaemic stroke [3]. However, due to a short therapeutic window (4.5 h of stroke onset), stringent eligibility criteria, and the increased risk of haemorrhage beyond this time point, globally <1% of ischaemic stroke patients benefit from this treatment each year [4]. Considering that many novel compounds failed to replicate the favourable outcomes from experimental studies into clinical trials, a large number of studies have proposed cell-based therapies as alternative approaches for stroke [5-7]. Cells can better respond to temporal and spatial changes affecting their environment after an ischaemic attack by interacting with other cells and synthesising various biologically active substances to promote neurovascular regeneration [8]. Amongst all the cell-based strategies, the one that utilises a functional subtype of endothelial progenitor cells (EPCs), namely outgrowth endothelial cells (OECs), may be the most promising therapeutic option in post-ischaemic restoration of neurovascular integrity due to their unique capacity to detect and repair endothelial damage, the main cellular component of blood-brain barrier (BBB) [9]. As deterioration of BBB integrity precedes vasogenic oedema and haemorrhagic transformation, the main causes of death within the first week of an ischaemic stroke, it is of vital importance to urgently restore the functionality of this unique barrier to minimise the risk of mortality and disability [10,11]. In this context, our recent study assessing the restorative effect of OECs on endothelium, damaged by wound scratch, has demonstrated that exogenous OECs effectively home into the site of injury and repair overall integrity of a well-established *in vitro* model of human BBB composed of human brain microvascular endothelial cells (HBMECs), astrocytes, and pericytes [12].

As a logical continuation of that study, the current study further investigates the barrier-restorative impacts of OECs in *in vitro* and *in vivo* settings of cerebral ischaemic injury using the abovementioned BBB model and a rodent model of human middle cerebral artery occlusion (MCAO), respectively. It also investigates the molecular mechanism involved in the barrier-protective effects of OECs.

Material and methods

Cell culture

HBMECs, pericytes, and astrocytes were purchased from TCS CellWorks Ltd. (Buckingham, UK) and were cultured in a humidified atmosphere (75% N₂, 20% O₂, 5% CO₂) at 37°C with their respective media (ScienCell Research Laboratories, San Diego, USA). To create ischaemia-reperfusion injury *in vitro*, cells were exposed to 4 h oxygen-glucose deprivation alone or followed by 20 h reperfusion (OGD±R) in the absence or presence of exogenously added OECs. OECs were isolated from mononuclear cells obtained from a 30-ml of human peripheral blood sample, and were cultured on fibronectin-coated well plates as before [12]. The EBM-2 medium (Lonza) containing 20% FBS and all required supplements provided with the media were used to grow the OECs. Visual inspection of cobblestone morphology is used to initially identify the OEC phenotype and indicate appropriate stem cell differentiation. The cell morphology figures were acquired by using 10x magnification and 0.25 numerical aperture. The experimenters were aware of the experimental groups.

Establishment of triple cell co-culture model of human BBB

An *in vitro* model of human BBB was established by simultaneous culture of HBMECs, astrocytes, and pericytes [13]. Briefly, approximately 7.5×10^4 of astrocytes were seeded on the basal side of polyester Transwell inserts (0.4 µm pore size, 12 mm diameter polyester membrane, High Wycombe, UK), which were subsequently inverted to return to their original orientation, once the cells were attached to the surface of the Transwell insert. 4×10^4 HBMECs,

OECs, or combination of both cells (ratio 2:1 in favour of HBMECs) were seeded on the apical compartment of the insert and were left to grow until fully confluent. These Transwell inserts were eventually transferred to 12-well plates containing confluent pericytes, to set up the triple-culture model of human BBB. In some experiments, 10^4 of OECs were added to the apical side of the insert before exposure to OGD±R injury.

Assessment of BBB integrity and function

The integrity and function of the BBB were investigated by measuring the transendothelial electrical resistance (TEER, World Precision Instruments, Hertfordshire, UK) and paracellular flux of the low molecular weight permeability marker, sodium fluorescein (NaF, 376Da), respectively as before [12].

***In vivo* cerebral ischaemia**

Focal ischemia was induced in anaesthetised male Wistar rats by transient MCAO. A 4-0 round tip and silicon coated suture was inserted from the left common carotid artery into the internal carotid artery until reaching the circle of Willis to occlude the origin of the MCA. This technique avoids transection of the external carotid artery, improves welfare and prevents confounding effects on behavioural outcomes. Reperfusion was allowed after 60 minutes of occlusion to mimic the commonly encountered clinical sequence of thrombotic occlusion of a major vessel followed by reestablishment of blood flow. Cerebral blood flow (CBF) was measured by laser Doppler technique. Animals exhibiting >65% reduction in CBF during MCAO followed by >80% recovery after 10 minutes of reperfusion were included in the study. During the surgery and recovery periods, rectal temperature was monitored and kept at ~37°C. 24 h after the induction of MCAO, the animals were randomly divided into two subgroups and given either 4×10^6 OECs or vehicle (500 μ l in EBM-2 media) via tail vein injection. On day 4 of ischaemic injury (or on day 3 of OEC treatment), animals were sacrificed and their brains were removed and cut into three pieces: right and left cerebral hemispheres and cerebellum.

The presence of cerebral oedema was verified in ipsilateral and contralateral brain hemispheres via the wet-dry method. For this, brain samples were immediately weighed on an electronic balance to obtain their wet weight before drying them in an oven at 100°C for 24 h to obtain their dry weight. The % of brain water content (BWC) was calculated using the following formula: $BWC = [(wet\ weight - dry\ weight) / wet\ weight] \times 100\%$. The experimenters were blinded to the treatment the rats had received prior to all subsequent analyses.

All animal experiments have been carried out in accordance with the U.K. Animals (Scientific Procedures) Act, 1986 and associated guidelines, EU Directive 2010/63/EU for animal experiments.

Measurement of NADPH oxidase capacity and superoxide anion level

NADPH oxidase activity and superoxide anion production were assessed through lucigenin chemiluminescence and cytochrome C reduction assay, as previously described [14].

Proliferation assay

The proliferation capacity of the cells was assessed by using the 4-[3-(4-Iodophenyl)-2-(4-nitrophenyl)-2H-5-tetrazolium]-1.3-benzene disulfonate (WST-1) kit (Roche, Mannheim, Germany), according to the manufacturer's instructions. This measurement principally quantifies the cleavage of tetrazolium salt WST-1 by mitochondrial dehydrogenases in viable cells. So, the greater absorbance readings reflect the larger number of viable cells. Briefly, cells (5×10^3) were cultured in 96-well plates in a humidified atmosphere, as described above. After 48 h, the cells were subjected to experimental conditions, and the media were subsequently replaced with 100 μ L fresh medium containing 10 μ L of WST-1. The plates were incubated for 2 h at 37°C prior to reading the absorbance (450 nm) using a FLUOstar Omega plate reader (BMG Labtech Ltd., UK). The cell growth was also counted in a Neubauer chamber. The cells (5×10^3) were seeded in 6 well plate, harvested by trypsinisation, and counted every 48 hours.

The population doubling time (PDT) was computed by the following formula. The mean PDT of each time point was determined as the population doubling time for each cell-type.

$$PDT = \frac{t \times \log 2}{\log n_1 - \log n_2}$$

t: time period (hours)

n1: number of cells at harvested

n2: initial cell number

Migratory measurement

The migratory capacity of the cells was analysed using a modified Boyden chamber assay (Transwell inserts, 4.0µm pore size, Corning). The cells were cultured in T25 flasks until reaching 90% confluence. The medium then was replaced with migration medium (EBM-2 medium without FBS and supplements) containing 10 µg/mL Calcein (Calbiochem). After 2 h, the cells (5×10^4) were trypsinised and seeded in the upper chamber and cultured with migration medium. In the lower chamber, fully supplemented EBM-2 medium containing 5 µL/mL vascular endothelial growth factor (VEGF, Fisher Scientific, Loughborough, UK) was added. The plate was read after 18 h incubation at 37°C by using luminometer at excitation 485 nm and emission 520 nm. The final reading was obtained after subtracting with the blanks.

Tube formation assay

48-well plates were pre-coated with 150 µL of growth factor-reduced Matrigel (BD Biosciences) for 30 minutes at 37°C. Equal numbers of HBMECs, OECs, or both (9×10^4 , ratio 2:1) were then seeded in the plates for 8 h. Tubule networks was visualised by a light microscope. Tube formation figures were captured using 4x magnification and 0.12 numerical aperture. The total number and length of tubule networks, defined by sum of number or length of segments, isolated elements, and branches detected in the analysed area, were assessed using ImageJ software (version 1.52k, NIH, Maryland, USA) [15].

Adhesion assay

96-well plates were pre-coated with fibronectin (1 mg/mL, Sigma) or collagen type I (0.4 mg/mL, Sigma), followed by incubation for 1 h at 37°C. The plates were then washed with PBS, and the cells (10^4) were seeded in the pre-coated plates. After 1 h incubation at 37°C, the plates were washed again and examined under light microscope. The adherent cells were counted in at least four random fields per well. The images were acquired using 10x magnification and 0.25 numerical aperture.

Immunocytochemistry

Cells (5×10^4) were seeded on fibronectin-coated (1 mg/mL, Sigma) coverslips using their specialised medium containing VEGF (5 μ L/mL, Fisher Scientific, Loughborough, UK). Once the cells reached 95% confluence, they were incubated with DiI-labelled acetylated-low density lipoprotein (DiI-Ac-LDL, 1 mg/mL, Invitrogen, Loughborough, UK) for 4 hours, and subsequently with FITC-conjugated Ulex europaeus agglutinin (FITC-UEA-1, 1 mg/mL, Sigma) for 2 hours. After that, the cells were fixed with 4% formaldehyde and mounted on glass slides using mounting medium (Vector Laboratories, Peterborough, UK). The figures were captured by using 10x magnification and 0.3 numerical aperture.

To detect ZO-1 localisation, identical numbers of HBMECs or OECs (9×10^4) were cultured on coverslips until they reach about 95% confluence. In some experiments, to distinguish between HBMECs and OECs, the latter was pre-labelled through incubation with DiI-Ac-LDL for 4 h at 37°C, and then co-cultured with HBMECs at a ratio of 1:2. The cells exposed to TNF- α (10 ng/mL) for 6 hours served as positive controls. Such concentration and time points were opted in the light of our previous time and concentration studies assessing the effect of this inflammatory mediator on cerebral barrier integrity and tight junction proteins [16]. Cells were then fixed and permeabilised with 4% paraformaldehyde for 20 minutes and 0.1% Triton X-100 for 5 minutes, respectively. Cells were subsequently blocked with 1% BSA, 22.52 mg/mL

glycine in PBST (PBS+ 0.1% Tween 20) before overnight exposure to ZO-1 antibody (1:250, Abcam) at 4°C, and their secondary antibody (1:250, Abcam) for 1 h at room temperature. Nuclei were detected by 4,6-diamidino-2-phenylindole staining, before visualising cells by fluorescence microscopy (Zeiss Axio Observer, Carl Zeiss Ltd, Cambridge, UK). The figures were acquired using 20x magnification and 0.17 numerical aperture. ImageJ software (version 1.52k, NIH, Maryland, USA) was used to quantify the fluorescence signal. The data were presented as corrected total cell fluorescence (CTCF), calculated by using the following formula and subsequently normalised by the number of cells displayed [17].

$$CTCF = A - (B \times C)$$

A: Integrated density

B: Area of selected cell

C: Mean fluorescence of background readings

Caspase 3/7 and cell viability assay

Apo-ONE homogeneous caspase-3/7 assay kit (Promega, Southampton, UK) and Calcein AM assay kit (Calbiochem) were used to measure caspase 3/7 activity and cell viability, respectively. Briefly, HBMECs (10^4) were grown on 96-well black opaque plates for 48 h. 5×10^3 OECs were added to the each well, and the plates were subjected to ischaemic injury for 4 h with glucose-free medium. To initiate the reaction, the medium was replaced with 100 μ L of caspase 3/7 assay buffer, containing the non-fluorescent caspase substrate, rhodamine 110, bis-(N-CBZL-aspartyl- L-glutamyl-L-valyl-L-aspartic acid amide; Z-DEVD-R110) or 100 μ L of Calcein AM/PBS (10 μ g/mL). Plates were immediately frozen at -80°C overnight, then they were completely thawed in a plate shaker for 2 h prior to reading the fluorescence (excitation/emission: 485/520 nm) using FLUOstar Omega plate reader (BMG Labtech Ltd.,

UK). Blanks were subtracted from the readings before normalising activity against mg protein. (Figure 7D) [18,19].

Statistical analyses

Data are displayed as mean \pm standard error of the mean (SEM) from a minimum of three independent experiments where “*n*” refers to biological replicates ($n, \geq 3$). Data were tested for normality using the Shapiro-Wilk normality test. Statistical analyses were performed by *t*-test, Mann Whitney, or one-way analysis of variance (ANOVA), followed by Tukey’s post hoc analysis. GraphPad Prism 8.4.3 statistical software package (GraphPad Software Inc., La Jolla, Ca, USA) was used to perform these analyses. $P < 0.05$ was considered as significant.

Results

OECs possess endothelial cell characteristics

Similar to HBMECs, OECs display typical cobblestone morphology, bind to FITC-UEA-1 and uptake Dil-Ac-LDL, suggesting that OECs possess true endothelial cell characteristics (Figure 1). We and others have previously shown that OECs isolated in this fashion also express specific markers for immaturity (CD133), stemness (CD34), and endothelial maturity (CD31), but not for hematopoietic cells (CD45) [12,20].

OECs display adequate adhesive capacity

As the homing process of OECs to the site of injury involves the adhesion of these progenitor cells to the extracellular matrix (ECM) [21], the current study comparatively investigated the capacity of OECs and resident ECs, namely HBMECs to adhere two different components of the ECM, fibronectin and collagen. The initial data showed that the application of fibronectin and collagen does not significantly affect the viability of both OECs and HBMECs (Supplementary Figure 1). The subsequent study then showed that both cells adhere to both ECM components in equal measures (Figure 2).

OECs possess higher migratory, proliferative, and anti-oxidant capacity

Time course assessment of cell growth has shown that, compared to HBMECs, OECs possess a greater proliferative capacity with shorter population doubling time (PDT) (Figure 3A, B). Scrutiny of proliferative and migratory capacities of OECs using WST-1 assay and Transwell inserts, respectively also show that OECs possess remarkably greater proliferative and migratory capacity compared to mature HBMECs (Figure 3C, D). Furthermore, compared to HBMECs, OECs are equipped with significantly higher basal total anti-oxidant capacity and lesser pro-oxidant NADPH oxidase activity as well as superoxide anion generation (Figure 3E-G).

OECs can integrate with HBMECs and form functional BBB

When cultured with pericytes and astrocytes, OECs alone or mixed with HBMECs form equally tight and functional BBB as those established with HBMECs, suggesting that OECs can help form a functional BBB on their own and/or through close interaction with resident brain endothelial cells (Figure 4). Immunocytochemical analyses of HBMECs, OECs, and HBMECs mixed with Dil-Ac-LDL-labelled OECs demonstrated the uninterrupted staining of tight junction protein ZO-1 between adjacent cells and confirmed the close interaction between resident and progenitor cells (Figure 5A and Supplementary Figure 2 for the positive control). Moreover, formation of coherent tubule networks on matrigel with HBMEC and OEC co-cultures further proved the capacity of OECs to fully integrate into vascular endothelium (Figure 5B). This is further substantiated by the quantification of the number and length of tubules as well as the intensity of ZO-1 staining for HBMECs, OECs and their co-cultures (Figure 5C-E).

Administration of OECs restores BBB integrity and function

Ultimately, the barrier-reparative effect of OECs was determined on a co-culture model of the BBB consisting of HBMECs, astrocytes, and pericytes. OGD substantially impaired BBB

integrity and function, as observed by the decreases in TEER and increases in sodium fluorescein flux, respectively (Figure 6A, B). Moreover, reperfusion markedly worsened the deleterious effect of OGD on BBB integrity and function and supported the findings of relevant previous studies [18,19]. However, treatments with OEC attenuated the impact of ischaemia-reperfusion injury on BBB and restored its integrity and function as evidenced by improved TEER and NaF flux readings, respectively.

Similarly, administration of OECs (4×10^6 cells) to a rodent model of human transient ischaemic stroke 24 h after induction of MCAO also led to significant decreases in ipsilateral, but not contralateral, oedema volumes on day 3 of treatment compared to vehicle-treated animals, implying that OECs can repair cerebral barrier damage by either direct incorporation into vasculature or through paracrine mechanisms or combination of both (Figure 6C).

Exogenous OECs attenuate oxidative stress and cell death

To provide a mechanistic understanding for the putative benefits achieved by treatments with OECs during ischaemic injury, the state of oxidative stress and cell death were assessed in HBMECs subjected to OGD injury in the absence or presence of OECs. While ischaemia substantially elevated NADPH oxidase activity and superoxide anion levels in HBMECs, the key elements related to oxidative stress, treatment with exogenous OECs reduced the level of both parameters to the levels observed in control groups (Figure 7A, B). In line with these findings, treatments with OECs also decreased the rate of cell death, as observed by the significant reduction in pro-apoptotic enzyme caspase 3/7 activities and improvements in HBMEC viability (Figure 7C, D).

Discussion

The BBB is formed by intimate interactions amongst BMECs, astrocytes, and pericytes. It controls the exchange of molecules between systemic circulation and the brain parenchyma to maintain the cerebral physiological function [22]. Since BBB damage constitutes the main

cause of death and neurological deterioration in the first week of ischaemic stroke, restoration of this distinctive barrier may be a very effective therapeutic strategy to mitigate stroke-related damage [23,24]. Re-endothelialisation of dead or dying cerebral vasculature not only relies on the lateral migration and proliferation of resident brain endothelial cells but also on the bioavailability of functional OECs, which can promote endothelial repair directly (through differentiation into endothelial cells) or indirectly (by releasing various paracrine elements) [9]. Strong associations observed between the availability and functionality of these particular stem cells, and the extent of infarct volume and neurological recovery, corroborate the pivotal role of OECs in the pathogenesis of ischaemic stroke and in determining the severity of post-ischaemic damages [25]. Moreover, these encouraging findings have led to consideration of new therapeutic strategies for ischaemic stroke where administration of a sufficient number of highly functional OECs is thought to help restore brain endothelial layer and maintain neurovascular integrity [26].

Data generated in the current study have shown that OECs possess endothelial cell characteristics, in that they display a typical cobblestone morphology, bind to specific lectin, endocytose Dil-Ac-LDL, and form well-established tubule networks on Matrigel. Hence, it is of no surprise that OECs successfully integrate into the cerebral vascular network, as shown by the coherent tube-like structure on Matrigel and the usual distribution of ZO-1, when co-cultured with HBMECs. The acquisition of similar TEER value and paracellular flux of *in vitro* models of human BBB established with HBMECs and OECs alone or together further corroborate that OECs can form structural and functional cerebral barriers. In addition, the markedly higher total anti-oxidant capacity and lower NADPH oxidase activity and superoxide anion level suggest that these cells may resist the hostile pathological microenvironment, and therefore may make effective therapeutics to restore cerebrovascular function during or after an ischaemic injury [27-29].

Through using one of the most clinically relevant *in vitro* models of human BBB, the current study has shown that exogenous addition of OECs during OGD±R effectively repairs BBB integrity and function, as attested by increases in TEER value and decreases in sodium fluorescein flux across the barrier, respectively. These barrier-reparative effects have also been replicated in *in vivo* settings. Namely, the intravenous administration of OECs 24 h after induction of MCAO led to marked decreases in ipsilateral, but not contralateral, brain water content on day 3 after treatment. These beneficial effects of OECs may in part be attributed to the effective homing of OECs to the site of injury, wherein they restore the integrity of neurovascular unit by either replacing the dead or damaged brain endothelial cells or secreting a number of vasoactive compounds [30]. It is important to note here that OECs were administered to stroke animals in this study well beyond the clinically recognised therapeutic window for thrombolysis (4.5 h of stroke onset). Given that globally >99% of ischaemic stroke patients do not receive thrombolytic therapy each year due to short therapeutic window, expense, issues relating to eligibility, lack of expertise, increased risk of haemorrhage beyond the acute phase of stroke, *etc*, these results are of utmost importance [4,9]. Nevertheless, it is important to consider the anatomical and physiological differences between rodent and human neurovasculature when extrapolating these results to a clinical study [31]. It is also important to remember that recovery from ischaemic stroke may be much faster in rodents than humans and thus the assessment of oedema volumes on day 3 of a rodent stroke may not easily be correlated with outcome measures assessed on day 90 or beyond in clinical settings [32].

Although low-level production of reactive oxygen species (ROS) is a prerequisite for neurovascular stability, their excessive availability stemming in large part from the overactivity of pro-oxidant enzyme NADPH oxidase is associated with endothelial dysfunction and neurovascular complications [33]. The decreased infarct volume and cerebral barrier damage observed in animal models of ischaemic stroke treated with specific NADPH oxidase

inhibitors, such as apocynin, Vas2870, or DPI, prior to occlusion of MCA substantiates the pivotal role played by this enzyme in the initiation and progression of ischaemic cerebral damage [34-37]. Substantial increases observed in NADPH oxidase activity and superoxide anion production in HBMEC subjected to OGD±R observed in the current study further support these findings. As co-treatment with OECs normalised the levels of both parameters in both settings, it is possible that modulation of oxidative stress and downstream target NF-κB may in part account for the neurovascular restorative effects of OECs [38].

Accumulating evidence indicate that apoptosis of brain endothelial cells aggravate ischaemic injury by compromising tight junction formation and thus microvascular integrity through stimulation of a range of mechanisms in particular that of NADPH oxidase-superoxide anion-caspase 3/7 signalling pathway [19,39,40]. Examination of caspase-3/7 activity and cellular viability rate in the present study in HBMECs subjected to ischaemic injury has confirmed the importance of this pathway by showing significant increases in the activity of these pro-apoptotic enzymes alongside a decrease in HBMEC survivability. By also showing that exogenously added OECs suppress caspase-3/7 activity and increase HBMEC viability, this study also adds further weight to neurovascular restorative capacity of OECs. In addition to the regulation of caspase 3/7, suppression of pro-apoptotic proteins Bax expression and potentiation of anti-apoptotic Bcl-2 expression may also contribute to neurovascular protective effect of OECs against cerebral ischaemic injury-induced apoptosis [38,41].

Despite showing a remarkably proliferative potential, after a certain number of replications OECs start manifesting the signs of senescence at morphological, structural and functional levels as ascertained by the appearance of flattened and enlarged morphology, nuclear damage, and limited proliferative and migratory capacity. Hence, understanding the molecular mechanisms involved in this process is of paramount importance to generate a large number of highly functional homogenous OECs that can be used as therapeutics and also to regulate the

bioavailability of those are already present in circulation [42]. Considering that increases in oxidative stress constitutes one of the major driving forces in endothelial senescence, the modulation of key factors associated with this phenomenon such as pro-oxidant and anti-oxidant enzymes may delay OEC senescence and as a consequence enhance their vasoreparative function [43].

Transplantation of cells to the same individual who donated the cells (autologous therapy) is regarded as the best option for cell-based therapies, due to diminished risk of immunological reactions, biological incompatibility, and disease transmission [44]. However, the requirement for a prolonged period of time, weeks if not months, to prepare sufficient number of clinical grade autologous cells, and possible dysfunctionality of OECs isolated from patients may render application of these cells in acute ischaemic stroke settings impossible [45,46]. Hence, allogeneic cell therapy, involving administration of *ex vivo* expanded cells to an unrelated recipient, may address these pitfalls and offer several advantages. Firstly, allogeneic therapeutic options allow isolation of highly functional cells from young and healthy donors which can then be subjected to multiple quality control strategies as well as to pharmacological, epigenetic, and genetic manipulation in an effort to enhance their vasoreparative function before administration to patients [47]. Secondly, the cells can be expanded in large quantities and cryopreserved [48]. Thirdly, expression of inherently higher levels of anti-inflammatory factors (e.g. IL-10 and TGF- β) and immunoregulator molecules such as HLA-G may render OECs very safe therapeutics due to expected absence of severe inflammatory reactions. In support of this, no adverse effects have been reported in ischaemic models of dorsal chamber immunocompetent mouse model transplanted with these stem cells [49]. The observation of no clinical abnormalities, cell toxicity, and tumorigenesis in healthy dog or mouse model of ischaemic retinopathies administered with human umbilical cord-derived OECs further substantiate this notion, and confirm the safety of allogeneic therapeutic approach [50,30].

Nevertheless, pre-clinical assessment and optimisation of OEC dose, route of administration, and effective time window is urgently needed to determine efficacy (in the context of regenerating damaged tissues and improving neurological function) and safety (risk of tumour formation and immunological reactions), as a prerequisite to develop off-the-shelf allogenic cell products for ischaemic stroke patients.

In conclusion, this study has shown that exogenous addition of OECs following cerebral ischaemic injury can effectively repair BBB damage and suppress brain oedema formation in part by suppressing oxidative stress and resident cell apoptosis.

Declarations

Funding

This study was supported by a grant to Dr Bayraktutan from The Dunhill Medical Trust (R459/0216) and funding from Doctoral Training Program of LPDP (Indonesian Endowment Fund for Education), Ministry of Finance, Republic of Indonesia.

Conflict of Interest

The authors declare that there are no conflicts of interest.

Data Availability

The datasets used and analysed during the current study are available from the corresponding author on reasonable request.

Authors Contributions

RRA and MA equally contributed to all experiments and data analysis. RRA wrote the first draft of the manuscript. U.B. designed and supervised the study, interpreted the data and wrote the manuscript. All authors approved the final version for publication.

References

1. Roth GA, Abate D, Abate KH et al. (2018) Global, regional, and national age-sex-specific mortality for 282 causes of death in 195 countries and territories, 1980-2017: a systematic analysis for the Global Burden of Disease Study 2017. *The Lancet* 392 (10159):1736-1788. doi:10.1016/S0140-6736(18)32203-7
2. Kyu HH, Abate D, Abate KH et al. (2018) Global, regional, and national disability-adjusted life-years (DALYs) for 359 diseases and injuries and healthy life expectancy (HALE) for 195 countries and territories, 1990-2017: a systematic analysis for the Global Burden of Disease Study 2017. *The Lancet* 392 (10159):1859-1922. doi:10.1016/S0140-6736(18)32335-3
3. Kadir RRA, Bayraktutan U (2020) Urokinase Plasminogen Activator: A Potential Thrombolytic Agent for Ischaemic Stroke. *Cellular and Molecular Neurobiology* 40 (3):347-355. doi:10.1007/s10571-019-00737-w
4. Kadir RRA, Alwjwaj M, Bayraktutan U (2020) MicroRNA: An Emerging Predictive, Diagnostic, Prognostic and Therapeutic Strategy in Ischaemic Stroke. *Cellular and Molecular Neurobiology*. doi:10.1007/s10571-020-01028-5
5. Chen X, Wang K (2016) The fate of medications evaluated for ischemic stroke pharmacotherapy over the period 1995-2015. *Acta Pharm Sin B* 6 (6):522-530. doi:10.1016/j.apsb.2016.06.013
6. Misra V, Ritchie MM, Stone LL et al. (2012) Stem cell therapy in ischemic stroke: role of IV and intra-arterial therapy. *Neurology* 79 (13 Suppl 1):S207-S212. doi:10.1212/WNL.0b013e31826959d2
7. Li Z, Dong X, Tian M et al. (2020) Stem cell-based therapies for ischemic stroke: a systematic review and meta-analysis of clinical trials. *Stem Cell Research & Therapy* 11 (1):252. doi:10.1186/s13287-020-01762-z

8. Sahota P, Savitz SI (2011) Investigational therapies for ischemic stroke: neuroprotection and neurorecovery. *Neurotherapeutics* 8 (3):434-451. doi:10.1007/s13311-011-0040-6
9. Bayraktutan U (2019) Endothelial progenitor cells: Potential novel therapeutics for ischaemic stroke. *Pharmacological Research* 144:181-191. doi:<https://doi.org/10.1016/j.phrs.2019.04.017>
10. Krueger M, Mages B, Hobusch C et al. (2019) Endothelial edema precedes blood-brain barrier breakdown in early time points after experimental focal cerebral ischemia. *Acta Neuropathologica Communications* 7 (1):17. doi:10.1186/s40478-019-0671-0
11. Jiang X, Andjelkovic AV, Zhu L et al. (2018) Blood-brain barrier dysfunction and recovery after ischemic stroke. *Prog Neurobiol* 163-164:144-171. doi:10.1016/j.pneurobio.2017.10.001
12. Abdulkadir RR, Alwjaj M, Othman OA et al. (2020) Outgrowth endothelial cells form a functional cerebral barrier and restore its integrity after damage. *Neural Regen Res* 15 (6):1071-1078. doi:10.4103/1673-5374.269029
13. Shao B, Bayraktutan U (2013) Hyperglycaemia promotes cerebral barrier dysfunction through activation of protein kinase C- β . *Diabetes Obes Metab* 15 (11):993-999. doi:10.1111/dom.12120
14. Kadir RRA, Alwjaj M, McCarthy Z et al. (2021) Therapeutic hypothermia augments the restorative effects of PKC- β and Nox2 inhibition on an in vitro model of human blood-brain barrier. *Metabolic Brain Disease*. doi:10.1007/s11011-021-00810-8
15. Chevalier F, Lavergne M, Negroni E et al. (2014) Glycosaminoglycan mimetic improves enrichment and cell functions of human endothelial progenitor cell colonies. *Stem Cell Research* 12 (3):703-715. doi:<https://doi.org/10.1016/j.scr.2014.03.001>

16. Abdullah Z, Bayraktutan U (2014) NADPH oxidase mediates TNF- α -evoked in vitro brain barrier dysfunction: roles of apoptosis and time. *Mol Cell Neurosci* 61:72-84. doi:10.1016/j.mcn.2014.06.002
17. Migneault F, Dieudé M, Turgeon J et al. (2020) Apoptotic exosome-like vesicles regulate endothelial gene expression, inflammatory signaling, and function through the NF- κ B signaling pathway. *Scientific Reports* 10 (1):12562. doi:10.1038/s41598-020-69548-0
18. Abdullah Z, Rakkar K, Bath PMW et al. (2015) Inhibition of TNF- α protects in vitro brain barrier from ischaemic damage. *Molecular and Cellular Neuroscience* 69:65-79. doi:<https://doi.org/10.1016/j.mcn.2015.11.003>
19. Rakkar K, Bayraktutan U (2016) Increases in intracellular calcium perturb blood–brain barrier via protein kinase C- α and apoptosis. *Biochimica et Biophysica Acta (BBA) - Molecular Basis of Disease* 1862 (1):56-71. doi:<https://doi.org/10.1016/j.bbadis.2015.10.016>
20. Medina RJ, O'Neill CL, Humphreys MW et al. (2010) Outgrowth Endothelial Cells: Characterization and Their Potential for Reversing Ischemic Retinopathy. *Investigative Ophthalmology & Visual Science* 51 (11):5906-5913. doi:10.1167/iovs.09-4951
21. Zhao J, Mitrofan C-G, Appleby SL et al. (2016) Disrupted Endothelial Cell Layer and Exposed Extracellular Matrix Proteins Promote Capture of Late Outgrowth Endothelial Progenitor Cells. *Stem Cells Int* 2016:1406304-1406304. doi:10.1155/2016/1406304
22. Zhang W, Zhu L, An C et al. (2020) The blood brain barrier in cerebral ischemic injury – Disruption and repair. *Brain Hemorrhages* 1 (1):34-53. doi:<https://doi.org/10.1016/j.hest.2019.12.004>
23. Alwjaj M, Kadir RRA, Bayraktutan U (2021) The secretome of endothelial progenitor cells: a potential therapeutic strategy for ischemic stroke. *Neural Regen Res* 16 (8):1483-1489. doi:10.4103/1673-5374.303012

24. Bernardo-Castro S, Sousa JA, Brás A et al. (2020) Pathophysiology of Blood–Brain Barrier Permeability Throughout the Different Stages of Ischemic Stroke and Its Implication on Hemorrhagic Transformation and Recovery. *Frontiers in Neurology* 11:1605
25. Kukumberg M, Zaw AM, Wong DHC et al. (2020) Characterization and Functional Assessment of Endothelial Progenitor Cells in Ischemic Stroke Patients. *Stem Cell Reviews and Reports*. doi:10.1007/s12015-020-10064-z
26. Moubarik C, Guillet B, Youssef B et al. (2011) Transplanted late outgrowth endothelial progenitor cells as cell therapy product for stroke. *Stem Cell Rev Rep* 7 (1):208-220. doi:10.1007/s12015-010-9157-y
27. He T, Peterson TE, Holmuhamedov EL et al. (2004) Human endothelial progenitor cells tolerate oxidative stress due to intrinsically high expression of manganese superoxide dismutase. *Arteriosclerosis, thrombosis, and vascular biology* 24 (11):2021-2027. doi:10.1161/01.ATV.0000142810.27849.8f
28. Dernbach E, Urbich C, Brandes RP et al. (2004) Antioxidative stress-associated genes in circulating progenitor cells: evidence for enhanced resistance against oxidative stress. *Blood* 104 (12):3591-3597. doi:10.1182/blood-2003-12-4103
29. Sattler M, Winkler T, Verma S et al. (1999) Hematopoietic growth factors signal through the formation of reactive oxygen species. *Blood* 93 (9):2928-2935
30. Reid E, Guduric-Fuchs J, O'Neill CL et al. (2018) Preclinical Evaluation and Optimization of a Cell Therapy Using Human Cord Blood-Derived Endothelial Colony-Forming Cells for Ischemic Retinopathies. *Stem Cells Transl Med* 7 (1):59-67. doi:10.1002/sctm.17-0187
31. Hoshi Y, Uchida Y, Tachikawa M et al. (2013) Quantitative atlas of blood-brain barrier transporters, receptors, and tight junction proteins in rats and common marmoset. *J Pharm Sci* 102 (9):3343-3355. doi:10.1002/jps.23575

32. Corbett D, Carmichael ST, Murphy TH et al. (2017) Enhancing the alignment of the preclinical and clinical stroke recovery research pipeline: Consensus-based core recommendations from the Stroke Recovery and Rehabilitation Roundtable translational working group. *Int J Stroke* 12 (5):462-471. doi:10.1177/1747493017711814
33. Allen CL, Bayraktutan U (2009) Oxidative stress and its role in the pathogenesis of ischaemic stroke. *Int J Stroke* 4 (6):461-470. doi:10.1111/j.1747-4949.2009.00387.x
34. Nagel S, Genius J, Heiland S et al. (2007) Diphenyleneiodonium and dimethylsulfoxide for treatment of reperfusion injury in cerebral ischemia of the rat. *Brain Res* 1132 (1):210-217. doi:10.1016/j.brainres.2006.11.023
35. Zehendner CM, Librizzi L, Hedrich J et al. (2013) Moderate hypoxia followed by reoxygenation results in blood-brain barrier breakdown via oxidative stress-dependent tight-junction protein disruption. *PLoS One* 8 (12):e82823. doi:10.1371/journal.pone.0082823
36. Kleinschnitz C, Grund H, Wingler K et al. (2010) Post-stroke inhibition of induced NADPH oxidase type 4 prevents oxidative stress and neurodegeneration. *PLoS Biol* 8 (9). doi:10.1371/journal.pbio.1000479
37. Tang XN, Cairns B, Cairns N et al. (2008) Apocynin improves outcome in experimental stroke with a narrow dose range. *Neuroscience* 154 (2):556-562. doi:10.1016/j.neuroscience.2008.03.090
38. Qiu J, Li W, Feng S et al. (2013) Transplantation of bone marrow-derived endothelial progenitor cells attenuates cerebral ischemia and reperfusion injury by inhibiting neuronal apoptosis, oxidative stress and nuclear factor- κ B expression. *Int J Mol Med* 31 (1):91-98. doi:10.3892/ijmm.2012.1180
39. Park S, Kim JA, Choi S et al. (2010) Superoxide is a potential culprit of caspase-3 dependent endothelial cell death induced by lysophosphatidylcholine. *J Physiol Pharmacol* 61 (4):375-381

40. Chignalia AZ, Weinberg G, Dull RO (2020) Norepinephrine Induces Lung Microvascular Endothelial Cell Death by NADPH Oxidase-Dependent Activation of Caspase-3. *Oxid Med Cell Longev* 2020:2563764. doi:10.1155/2020/2563764
41. Hong Y, Yu Q, Kong Z et al. (2020) Exogenous endothelial progenitor cells reached the deficient region of acute cerebral ischemia rats to improve functional recovery via Bcl-2. *Cardiovasc Diagn Ther* 10 (4):695-704. doi:10.21037/cdt-20-329
42. Medina RJ, O'Neill CL, O'Doherty TM et al. (2013) Ex Vivo Expansion of Human outgrowth Endothelial Cells Leads to IL-8-Mediated Replicative Senescence and Impaired Vasoreparative Function. *STEM CELLS* 31 (8):1657-1668. doi:<https://doi.org/10.1002/stem.1414>
43. Coluzzi E, Leone S, Sgura A (2019) Oxidative Stress Induces Telomere Dysfunction and Senescence by Replication Fork Arrest. *Cells* 8 (1):19. doi:10.3390/cells8010019
44. Fang J, Guo Y, Tan S et al. (2019) Autologous Endothelial Progenitor Cells Transplantation for Acute Ischemic Stroke: A 4-Year Follow-Up Study. *Stem Cells Transl Med* 8 (1):14-21. doi:10.1002/sctm.18-0012
45. Fadini Gian P, Sartore S, Albiero M et al. (2006) Number and Function of Endothelial Progenitor Cells as a Marker of Severity for Diabetic Vasculopathy. *Arteriosclerosis, Thrombosis, and Vascular Biology* 26 (9):2140-2146. doi:10.1161/01.ATV.0000237750.44469.88
46. Kot M, Baj-Krzyworzeka M, Szatanek R et al. (2019) The Importance of HLA Assessment in "Off-the-Shelf" Allogeneic Mesenchymal Stem Cells Based-Therapies. *Int J Mol Sci* 20 (22). doi:10.3390/ijms20225680
47. Faris P, Negri S, Perna A et al. (2020) Therapeutic Potential of Endothelial Colony-Forming Cells in Ischemic Disease: Strategies to Improve their Regenerative Efficacy. *Int J Mol Sci* 21 (19):7406. doi:10.3390/ijms21197406

48. Reinisch A, Hofmann NA, Obenauf AC et al. (2009) Humanized large-scale expanded endothelial colony-forming cells function in vitro and in vivo. *Blood* 113 (26):6716-6725. doi:<https://doi.org/10.1182/blood-2008-09-181362>
49. Proust R, Ponsen AC, Rouffiac V et al. (2020) Cord blood-endothelial colony forming cells are immunotolerated and participate at post-ischemic angiogenesis in an original dorsal chamber immunocompetent mouse model. *Stem Cell Res Ther* 11 (1):172. doi:10.1186/s13287-020-01687-7
50. Lee SH, Ra JC, Oh HJ et al. (2019) Clinical Assessment of Intravenous Endothelial Progenitor Cell Transplantation in Dogs. *Cell Transplant* 28 (7):943-954. doi:10.1177/0963689718821686

Figure legends

Figure 1. Representative images of OECs characterisation. Immunocytochemistry studies have shown that OECs display typical cobblestone morphology, stain with FITC-UEA-1 and uptake Dil-Ac-LDL (A). Quantitative analyses of the signals, normalised by cell count, for FITC-UEA-1 and Dil-Ac-LDL show similar readings for HBMECs, OECs and the merged images (B). NS: not significant (*t*-test). $n \geq 4$. The morphology figures were acquired by using 10x magnification and 0.25 numerical aperture. Immunocytochemistry figures were obtained by using 10x magnification and 0.3 numerical aperture. Scale bar: 100 μm .

Figure 2. Representative images showing the capacity of HBMECs and OECs to adhere ECM components, fibronectin, and collagen observed under light microscope (A). Similar number of HBMECs and OECs appeared to attach ECM (B). NS: not significant (*t*-test for fibronectin and Mann-Whitney test for collagen). $n \geq 3$. The images were captured using 10x magnification and 0.25 numerical aperture. Scale bar: 100 μm .

Figure 3. Scrutiny of the HBMEC and OEC growth, using a Neubauer chamber, shows that OECs possess a faster proliferation rate and shorter population doubling time (PDT) (A – B). The levels of cell proliferation (WST-1 assay), migration (Boyden chamber assay), total anti-oxidant capacity (ELISA), NADPH oxidase activity (lucigenin chemiluminescence assay), and superoxide anion production (cytochrome *C* measurement) were assessed in HBMECs and OECs using the specific assays indicated in brackets. OECs display remarkably higher proliferative (C), migratory (D), and anti-oxidant capacity (E), but possess lower NADPH oxidase activity (F) and superoxide anion level (G). * $p < 0.05$, ** $p < 0.01$, and *** $p < 0.001$ (*t*-test). $n \geq 4$.

Figure 4. Schematic diagram of *in vitro* models of human BBB (A). TEER and paracellular flux of permeability marker sodium fluorescein were employed to study the integrity and function of BBB models, respectively. OECs, HBMECs, and OECs co-cultured with HBMECs

form equally tight and functional BBB as shown by the similar readings obtained for TEER (B) and paracellular flux (C). NS: not significant (ANOVA followed by Tukey's post hoc analysis). $n \geq 4$.

Figure 5. Immunocytochemistry and tube formation assay show that OECs, HBMECs, and Dil-Ac-LDL-labelled OECs (indicated with white arrows) co-cultured with HBMECs form tight junctions as evidenced by an uninterrupted staining of tight junction protein, ZO-1 (A) and formation of tubules on Matrigel (B). Quantitative analyses of the signals, normalised by cell count, for ZO-1 (C) and number (D) and length (E) of tubule networks show similar readings for HBMECs, OECs, and HBMEC+OEC co-cultures. NS: not significant (ANOVA followed by Tukey's post hoc analysis). $n \geq 4$. Immunocytochemistry figures were obtained using 20x magnification and 0.17 numerical aperture. Tubule network figures was acquired using 4x magnification and 0.12 numerical aperture. Scale bar: 50 μm .

Figure 6. Impact of post-ischaemic treatment with OECs on cerebral barrier in *in vitro* and *in vivo* settings. Treatment with OECs repair the integrity (A) and function (B) of an *in vitro* model of human BBB as evidenced by increases in TEER reading and decreases in paracellular flux, respectively. * $p < 0.05$, ** $p < 0.01$, and *** $p < 0.001$ (ANOVA followed by Tukey's post hoc analysis). $n \geq 4$. In line with these findings, intravenous administration of OECs 24 h after MCAO also decreased brain water content in the ipsilateral, but not in the contralateral, hemisphere of the brain, observed on day 3 after cellular treatment (C). *** $p < 0.001$ and NS: not significant (*t*-test). Four animals were studied in each group.

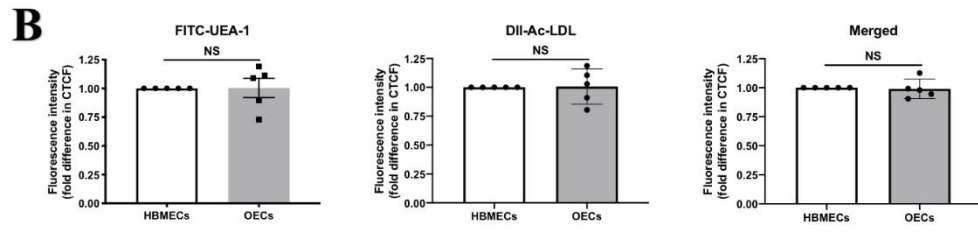
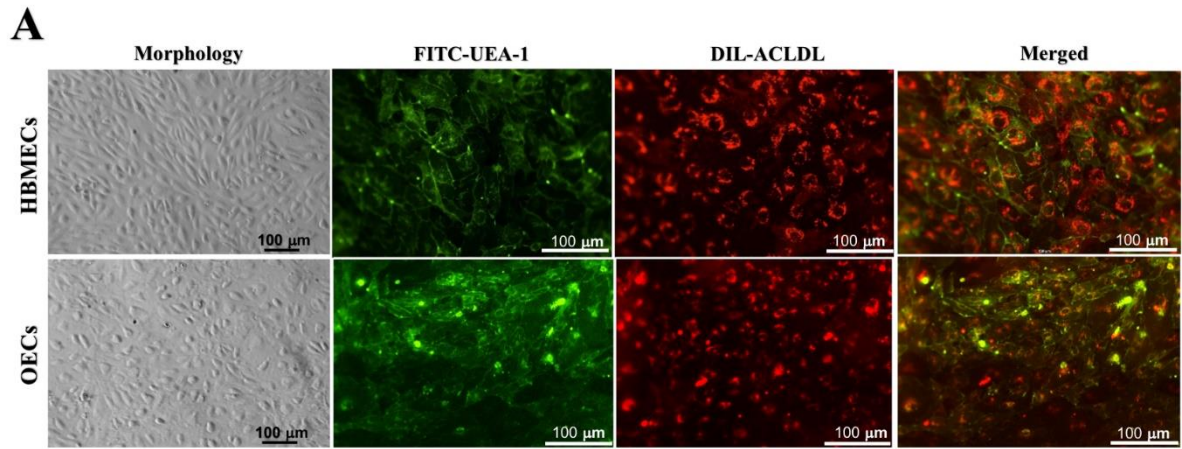
Figure 7. The effect of exogenous OECs on resident endothelial cell NADPH oxidase activity (lucigenin chemiluminescence assay), superoxide anion (cytochrome *C* measurement), caspase 3/7 activity (Apo-ONE homogeneous caspase-3/7 assay), and cell viability (Calcein AM assay) during experimental ischaemic injury. These parameters were assessed using the specific assays indicated in the bracket. Treatment with OECs effectively suppressed NADPH oxidase

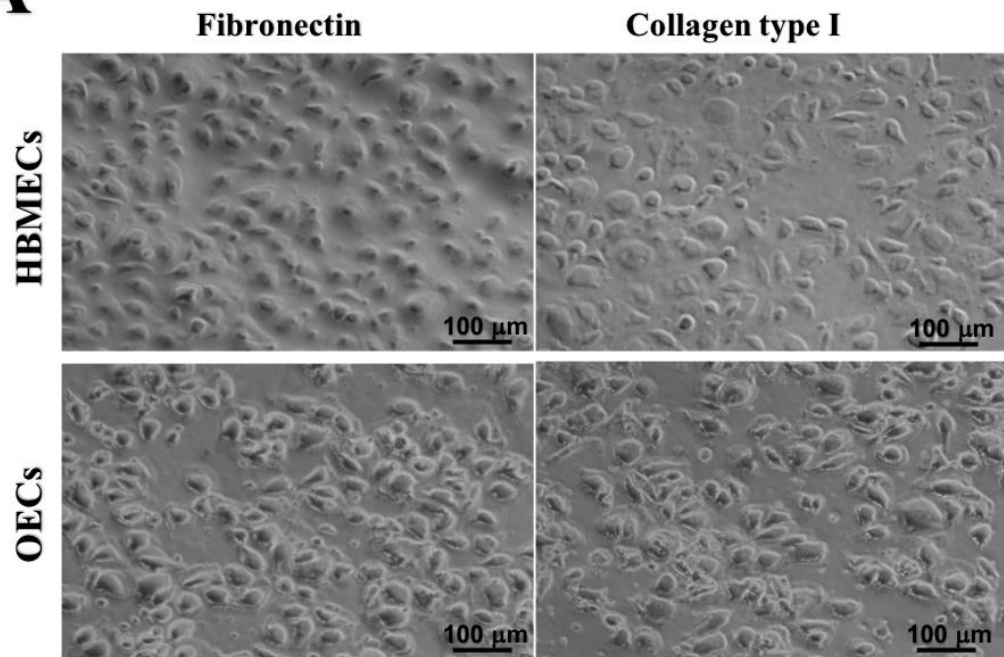
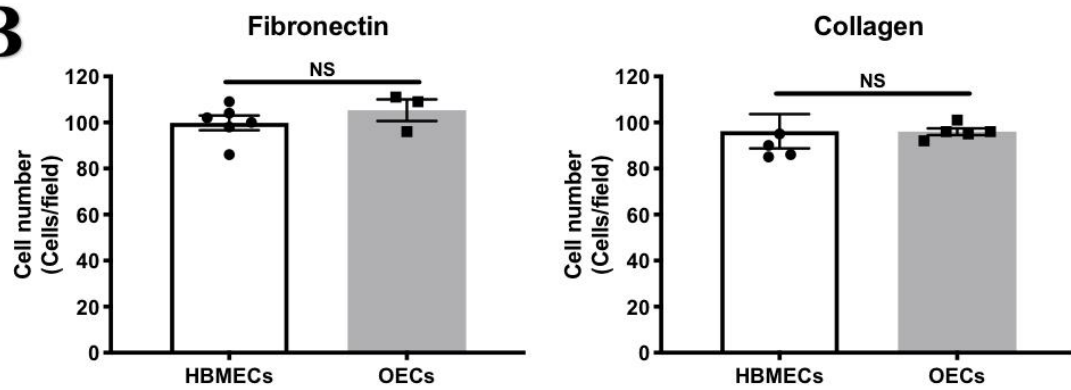
activity (A), superoxide anion level (B), and caspase 3/7 (C), while maintaining the cell viability (D) of resident brain endothelial cells subjected to oxygen-glucose deprivation (OGD). * $p < 0.05$ and *** $p < 0.001$ (t -test, Mann Whitney test or ANOVA followed by Tukey's post hoc analysis). $n \geq 4$.

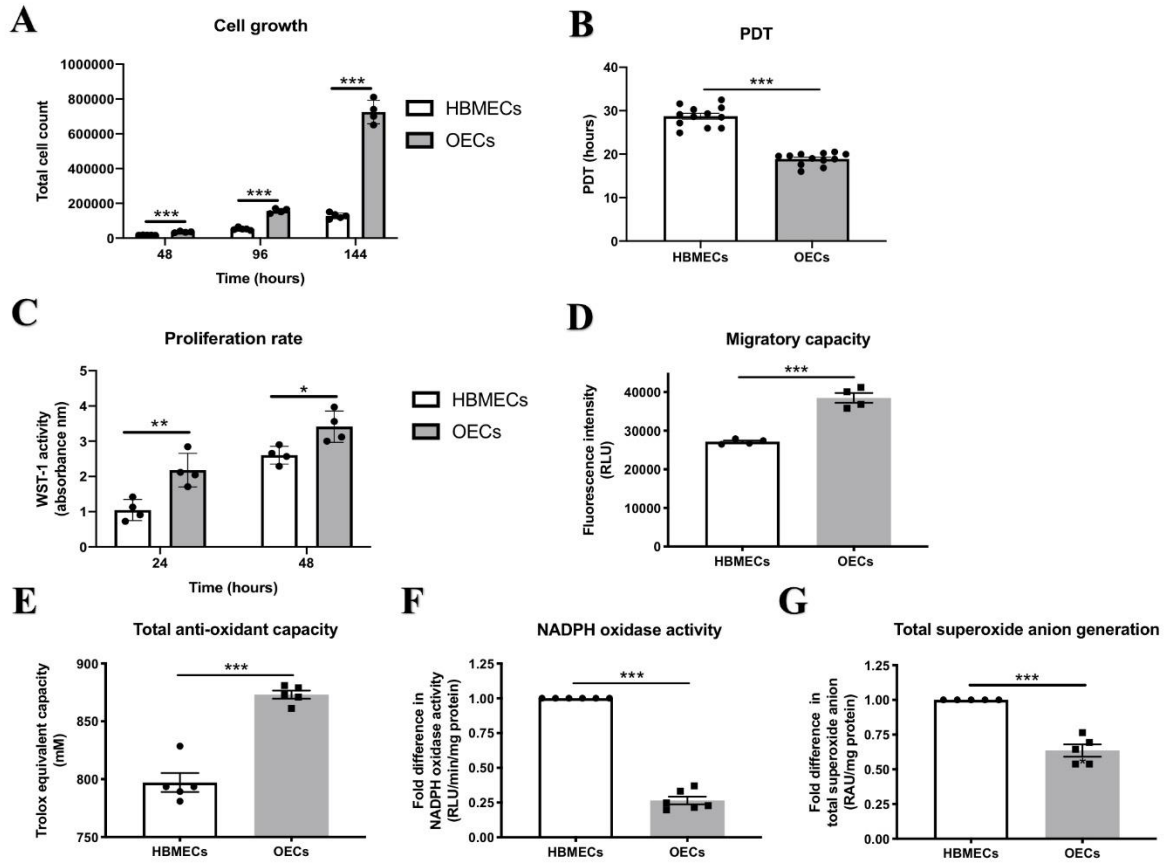
Legends for supplementary figures

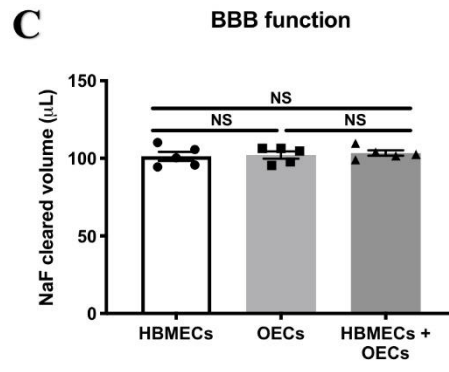
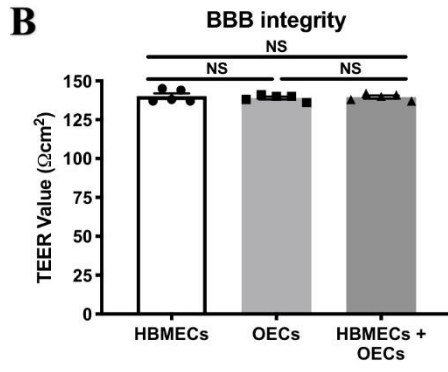
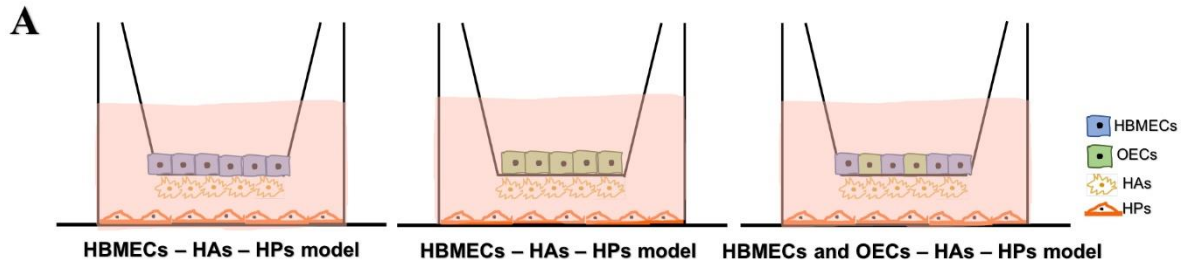
Figure 1. The effect of fibronectin or collagen coating on the viability of HBMECs (A) and OECs (B). Cellular viability, assessed by calcein AM assay, show similar readings for both HBMECs and OECs. NS: not significant (ANOVA followed by Tukey's post hoc analysis). $n = 4$.

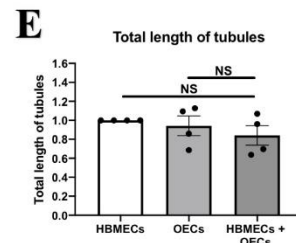
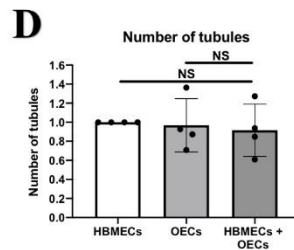
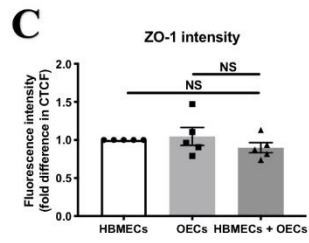
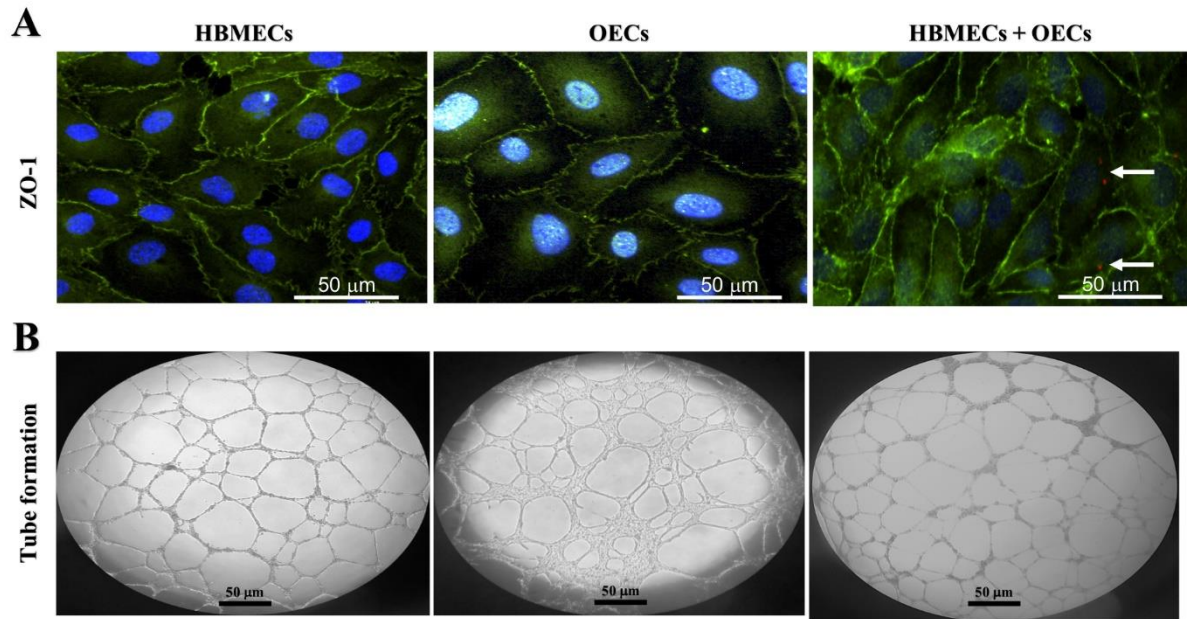
Figure 2. Intercellular distribution of tight junction protein ZO-1 in HBMECs and OECs in the absence or presence of TNF- α (10 ng/mL, 6 h) (A). TNF- α elicited significant decreases in ZO-1 fluorescence intensity in both HBMECs (B) and OECs (C). *** $p < 0.001$ (t -test). $n = 5$. The images were captured using 20x magnification and 0.17 numerical aperture. Scale bars: 50 μm .

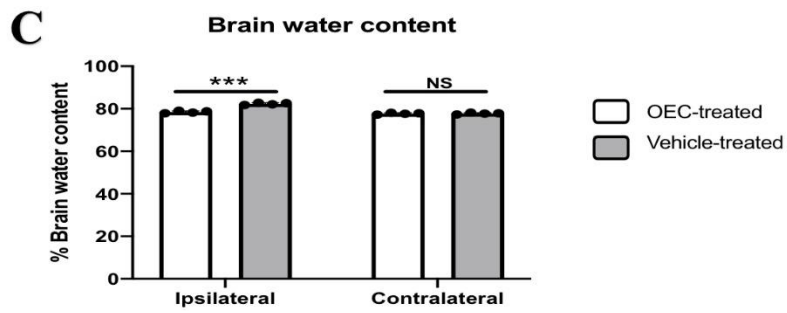
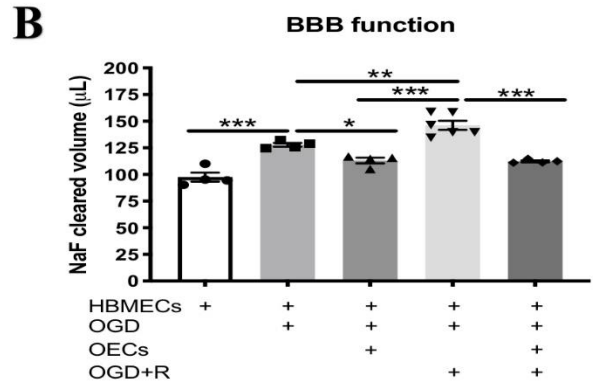
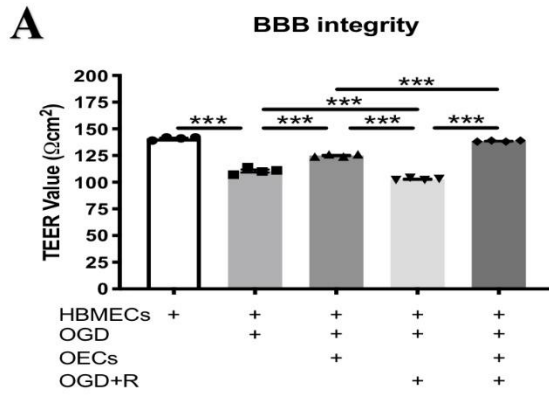


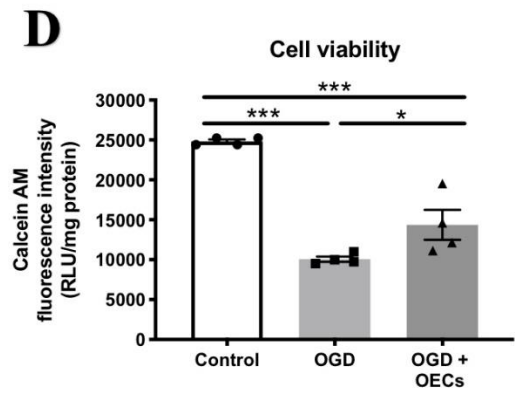
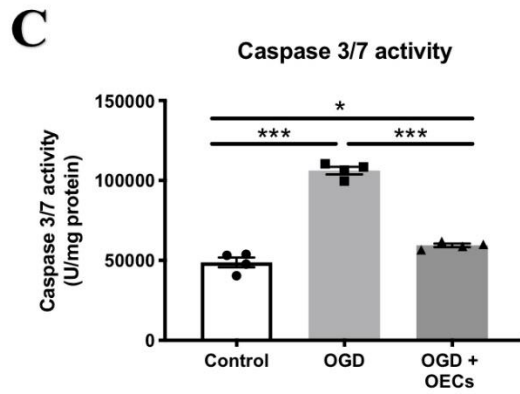
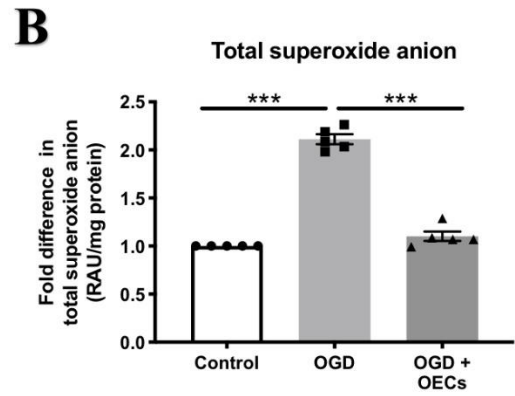
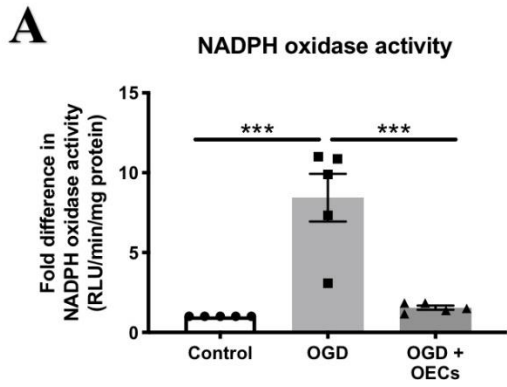
A**B**



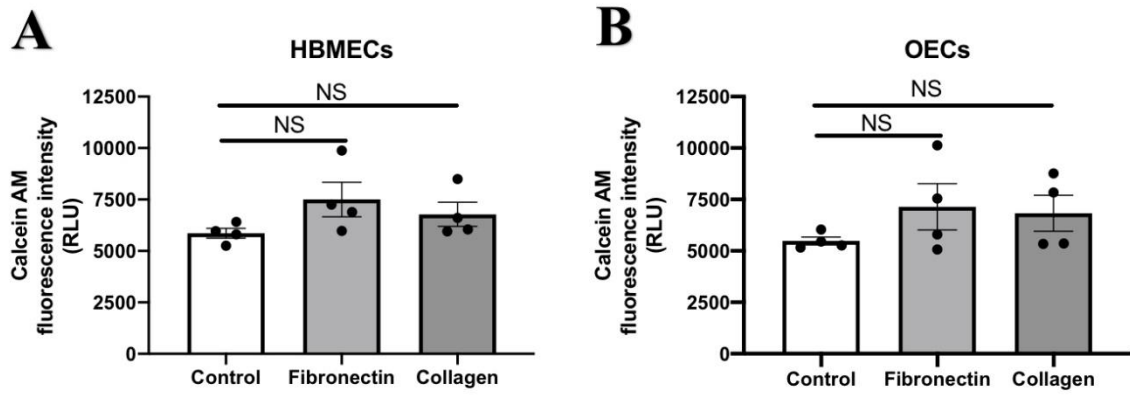








Supplementary figure 1



Supplementary figure 2

